


Estimation of population size and trends for highly mobile species with dynamic spatial distributions

Charlotte Boyd^{1,2}  | Jay Barlow² | Elizabeth A. Becker³ | Karin A. Forney^{3,4} |
Tim Gerrodette² | Jeffrey E. Moore² | André E. Punt¹

¹School of Aquatic and Fishery Sciences, University of Washington, Seattle, WA, USA

²Southwest Fisheries Science Center, National Marine Fisheries Service, National Oceanic and Atmospheric Administration, La Jolla, CA, USA

³Marine Mammal and Turtle Division, Southwest Fisheries Science Center, National Marine Fisheries Service, National Oceanic and Atmospheric Administration, Moss Landing, CA, USA

⁴Moss Landing Marine Laboratories, Moss Landing, CA, USA

Correspondence

Charlotte Boyd, School of Aquatic and Fishery Sciences, University of Washington, Seattle, WA, USA.

Email: boydchar@u.washington.edu

Editor: Helen Regan

Abstract

Aim: To develop a more ecologically realistic approach for estimating the population size of cetaceans and other highly mobile species with dynamic spatial distributions.

Location: California Current Ecosystem, USA.

Methods: Conventional spatial density models assume a constant relationship between densities and habitat covariates over some time period, typically a survey season. The estimated population size must change whenever total habitat availability changes. For highly mobile long-lived species, however, density–habitat relationships likely adjust more rapidly than population size. We developed an integrated population-redistribution model based on a more ecologically plausible alternative hypothesis: (1) population size is effectively constant over each survey season; (2) if habitat availability changes, then the population redistributes itself following an ideal free distribution process. Thus, the estimated relationship between densities and habitat covariates adjusts rather than population size. We constructed Bayesian hierarchical models corresponding to the conventional and alternative hypotheses and applied them to distance sampling data for Dall's porpoise (*Phocoenoides dalli*), a highly mobile cetacean with distribution patterns closely tied to cool sea-surface temperatures.

Results: The Dall's porpoise data provided strong support for the hypothesis based on an ideal free redistribution process. Our results indicate that the population size of Dall's porpoise within the survey region was relatively stable over each summer/fall survey season, but the distribution expanded and contracted with the extent of suitable habitat. Over multiple survey seasons, the model partitioned variation in observed densities among three sources: variation in population size, the density–habitat relationship and measurement error, leading to lower and more ecologically plausible estimates of interannual variation in population size.

Main conclusions: We conclude that the integrated population-redistribution model (IPRM) presented here represents an ecologically plausible model for use in future assessments of the population size and dynamics of cetaceans and other highly mobile long-lived species with variable spatial distributions.

KEYWORDS

Bayesian hierarchical model, California Current, Dall's porpoise, distance sampling, habitat model, spatial density model

1 | INTRODUCTION

Assessments of species' population size and trends are essential for effective conservation and management. However, abundance estimation is challenging for highly mobile species, especially those with dynamic spatial distributions linked to variation in the distribution of prey or suitable habitat (Ballance, 2007; Evans & Hammond, 2004; Forney, 2000; Nandintsetseg, Kaczensky, Ganbaatar, Leimgruber, & Mueller, 2016; Royle, Nichols, Karanth, & Gopalaswamy, 2009). Cetacean abundance estimates are commonly based on distance sampling data derived from line-transect surveys, but surveys often cover only a portion of the population's range and may take several months to complete. Spatially open populations may move in or out of the survey region depending on the distribution of suitable habitat, such that a variable proportion of the population is available for sampling in each survey or from one month to the next (Calambokidis & Barlow, 2004; Forney, 2000). This can lead to highly variable abundance estimates and impede efforts to estimate population size and trends. Moreover, estimates are difficult to interpret, as apparent increases or decreases in abundance may represent real changes in population size or mere shifts in distribution (Forney, 2000). This is a particular concern in regions where anthropogenic impacts to cetaceans are known or suspected. Our goal was therefore to develop and apply a more ecologically realistic modelling approach for estimating population size and trends for cetaceans or other highly mobile species with spatially dynamic distributions that vary with the distribution of suitable habitat.

Patterns of abundance and distribution in marine systems are determined in large part by oceanographic processes that vary at multiple spatial and temporal scales (Levin, 1992). In the California Current Ecosystem, for example, seasonal, interannual and multidecadal variation in oceanographic processes reconfigures entire food webs, from nutrient supply, through plankton and mid-trophic-level forage fish, to upper trophic-level consumers (Chavez, Ryan, Lluch-Cota, & Niquen, 2003; Santora, Schroeder, Field, Wells, & Sydeman, 2014). Even though cetacean habitat selection likely reflects the distribution of preferred prey, it can often be delineated in terms of static and/or dynamic environmental covariates, such as depth and sea-surface temperature, that serve as proxies for prey (see, e.g., Becker et al., 2010; Forney et al., 2012; Torres, Read, & Halpin, 2008).

Cetacean populations, being long-lived and highly mobile, generally respond spatially rather than demographically to changes in the abundance and distribution of their prey (Forney, 2000). Cetacean movement patterns vary widely. Some populations are resident year-round at consistently productive sites, and some undertake predictable long-distance migrations, while others exhibit less predictable and sometimes extensive seasonal or interannual distributional shifts in response to seasonal or interannual variation in the distribution of their prey and associated habitat (Stevick, McConnell, & Hammond, 2002). Here, we focus on the last of these.

We base our analysis on a case study of Dall's porpoise (*Phocoenoides dalli*). Dall's porpoise occurs throughout the North Pacific and adjacent seas (Morejohn, 1979). The species is generally

found in deeper waters over the continental shelf and slope, but also occurs farther offshore (Jefferson, 1988). It is considered a cold-temperate species, with distribution patterns closely tied to the distribution of cool sea-surface temperatures (typically <17–18°C) (Becker et al., 2010; Forney, 2000; Jefferson, 1988). This may reflect their need for the relatively high prey densities found in recently upwelled, nutrient-rich waters, characterized by cool surface temperatures. Dall's porpoise are probably opportunistic foragers, but feed primarily on small schooling fishes, squids and lanternfish (Jefferson, 1988). Previous studies have found evidence for interannual and seasonal shifts in distribution both north–south and inshore/offshore following the distribution of cool surface waters (e.g., Becker et al., 2014; Forney & Barlow, 1998; Henderson et al., 2014; Tynan et al., 2005), although the scale of individual movement patterns is not well known (Jefferson, 1988).

Conservation and management of cetaceans under the US Marine Mammal Protection Act (MMPA) is based on the “potential biological removal,” a function of estimates of population size, maximum population growth rate, and a “recovery factor” that depends on the status and trends of the population (Taylor, Wade, De Master, & Barlow, 2000; Wade, 1998). Two Dall's porpoise stocks are recognized in the US Exclusive Economic Zone—we focus on the stock that occurs in waters off Washington, Oregon and California (hereafter, the WA-OR-CA stock) (Carretta et al., 2017). Abundance estimates for this stock, based on distance sampling data from line-transect surveys in the California Current Ecosystem (CCE), are highly variable from one survey to the next (Barlow & Forney, 2007). Stock assessment and management is therefore based on multiyear averages across abundance estimates calculated separately for each survey year (Carretta et al., 2017). Trends in abundance have not been estimated to date. Some of the variation in abundance estimates has been attributed to shifts in the population's distribution in and out of the survey region in response to variable oceanographic conditions and methodological constraints (Forney, 2000; Forney & Barlow, 1998). The stock's range has not been delineated, but is assumed to extend well beyond the survey region (Figure 1a).

Forney (2000) suggested that variation in distribution patterns could be addressed by incorporating density–habitat relationships into models designed to estimate abundance and trends. However, this is difficult to achieve using conventional design-based distance sampling methods, for which inference rests on the assumption that the sampling scheme is random with respect to the underlying population distribution (Gregoire, 1998). In contrast, model-based approaches assume that the underlying distribution process can be described by a distribution model (Gregoire, 1998), and provide a framework for inference about the effects of habitat and other spatio-temporal covariates on population densities at much finer spatial and temporal scales (Conn et al., 2015; Johnson, Laake, & Hoef, 2010; Sillett, Chandler, Royle, Kéry, & Morrison, 2012).

Bayesian hierarchical models (BHM) provide new opportunities for model-based analysis of distance sampling data. Hierarchical models enable the joint estimation of an ecological process submodel that describes the ecological processes of interest (such as population size

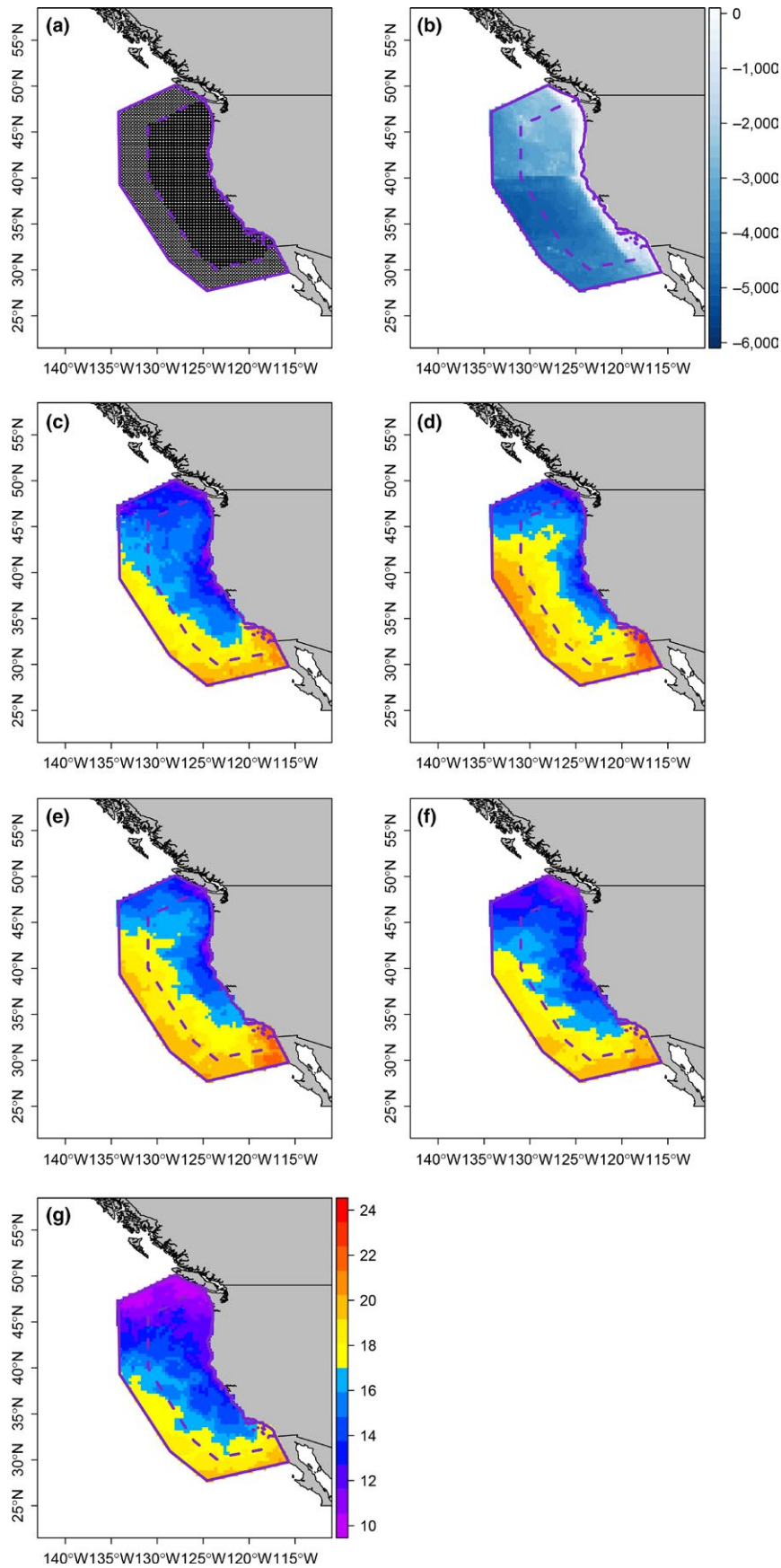


FIGURE 1 (a) California Current Ecosystem survey region (dashed purple line) and broader region (solid purple line) with centre points of 1/3-degree grid cells; (b) depth distribution (m); (c–g) monthly sea-surface temperature (°C) in July–November 2008. [Colour figure can be viewed at wileyonlinelibrary.com]

and distribution), and an observation submodel that describes the relationship between unobserved ecological state variables and the observed data (Royle & Dorazio, 2008). Moore and Barlow (2011, 2013, 2014) designed a series of BHM with ecological submodels for population dynamics to estimate population size and trends for fin whales (*Balaenoptera physalus*), beaked whales (family *Ziphiidae*) and sperm whales (*Physeter macrocephalus*) (see also Nadeem, Moore, Zhang, & Chipman, 2016). BHM designed to estimate distribution patterns as a function of habitat covariates have generally built on the multinomial N -mixture model developed by Royle, Dawson, and Bates (2004) (e.g., Chelgren, Samora, Adams, & McCreary, 2011; Gerrodette & Eguchi, 2011; Oedekoven et al., 2014). Pardo et al. (2015) developed multi-year models for blue whales (*Balaenoptera musculus*) and short-beaked common dolphins (*Delphinus delphis*), with an ecological submodel for the distribution process. Estimated densities at each sampling unit varied in direct response to temporal variation in the habitat covariate, leading to substantial interannual variation in the aggregate population size across the entire survey region. However, none of these models combine an aggregate population dynamics submodel and a distribution submodel incorporating habitat covariates.

A model that combines an aggregate population dynamics submodel with a habitat-based distribution submodel may improve inference about population sizes and trends for highly mobile populations that move across survey region boundaries in response to seasonal or interannual variation in the distribution of their prey and associated habitat. However, developing this model raises both ecological and methodological questions—how do populations redistribute themselves in response to variation in the distribution and quality of suitable habitat? And how can we capture these processes in an explicit hierarchical model?

Conventional spatial density models assume a constant relationship between population densities and habitat covariates over some time period, typically a survey season, which may extend over several months (e.g., Forney et al., 2012). If habitat availability changes during this period, then the estimated population size within the survey region must also change. Here, we develop an integrated population-redistribution model based on the alternative hypothesis that the modelled population size varies interannually, but is effectively constant over the course of each survey season and redistributes itself in proportion to suitable habitat within its range following an ideal free distribution process (Fretwell & Lucas, 1970). If the availability of suitable habitat varies over the survey season, the relationship between population density and habitat covariates adjusts rather than total population size.

We constructed three BHM representing these distinct hypotheses about population and distribution processes. We represented the conventional approach with a mixed-effects model (Model H0), in which the ecological process submodel comprises a fixed density-habitat relationship with random effects on year to allow for interannual variation in population size and habitat availability. There is no explicit submodel for the population process—instead, the population size within the survey region is inferred by integrating predicted densities over a fitted spatial density surface for the

survey region (as per Pardo et al., 2015). This mixed-effects model approximates the standard line-transect estimation process currently used to estimate Dall's porpoise abundance in the CCE survey region except that the survey region is not partitioned into strata (Barlow & Forney, 2007).

We developed an integrated population-redistribution model (IPRM) representing the alternative hypothesis (Model H1). In the IPRM, a population dynamics submodel is used to estimate changes in population size within the population's range between primary sampling occasions (e.g., survey years). A coupled distribution submodel is then used to estimate local densities in each sampling unit, assuming that the population is distributed in proportion to the relative availability of suitable habitat (i.e. habitat suitability at each location relative to habitat suitability throughout the range) on each secondary sampling occasion (e.g., survey months). This submodel is similar to the "closed-population ideal free" model developed by Conn et al. (2015) for a single survey year. We constructed two versions of the IPRM—a spatially closed model (Model H1a), in which the population's range coincides with the survey region; and a spatially open model (Model H1b), in which the population's range extends beyond the survey region.

We applied the three BHM to distance sampling data collected for Dall's porpoise in the CCE survey region in six survey years from 1991 to 2008. We chose Dall's porpoise for the case study because of their well-documented variation in spatial distribution as ocean conditions change at varying time-scales (Forney, 2000; Forney & Barlow, 1998), the strong habitat associations found in previous work (e.g., Becker et al., 2010, 2014), and because of the relatively large sample sizes (survey effort and sightings) available for model-building. We then used the three BHM to investigate (1) relative support for the different hypotheses on population and distribution processes for Dall's porpoise, and (2) the potential for IPRM that combine an aggregate population dynamics submodel with a habitat-based redistribution submodel to reduce variability and uncertainty in estimates of population size and trends for Dall's porpoise and other species whose distribution varies substantially based the distribution of suitable habitat, as proposed by Forney (2000).

2 | METHODS

2.1 | Distance sampling data

2.1.1 | Data collection

Vessel-based line-transect surveys for cetaceans were conducted by NOAA's Southwest Fisheries Science Center in the CCE during summer/fall of 1991, 1993, 1996, 2001, 2005 and 2008 (Figure 1a). Transect lines were arranged in a systematic grid to provide even coverage of the survey region over the course of each survey (Figure 1a). In 1991 and 1993, the survey region only covered waters off California, but it was expanded to waters off Oregon and Washington in subsequent years. The survey protocol was the same for all surveys (see Barlow & Forney,

2007; Kinzey, Olson, & Gerrodette, 2000). Research vessels travelled at approximately 10 kt along predetermined transect lines. Two experienced observers searched with pedestal-mounted 25× binoculars, each covering one quadrant from the ship's beam to the centre of the track-line from a port or starboard station on the flying bridge (approximately 10–15 m above sea level depending on the research vessel), while a third observer searched with unaided eyes and occasionally hand-held 7× binoculars from a central station. The third observer also recorded data on survey conditions and cetacean sightings, including species identification and estimated group size. Survey conditions, including Beaufort sea state, were recorded approximately every 30 min or whenever conditions changed.

2.1.2 | Data processing

Transect lines were partitioned into 10-km on-effort segments following the methods of Becker et al. (2010), and the following data were extracted for each segment ($j = 1 \dots J$): date; location of the segment mid-point; estimated Beaufort sea state ($B_{\text{segment},j}$); segment length (L_j); and number of groups of Dall's porpoise sighted (y_j). The average Beaufort sea state was used if the estimated Beaufort sea state changed during the course of a segment. Segments with Beaufort sea state >5 and sightings >4 km from the transect line were discarded following Barlow (2015).

The following data were extracted for each group of Dall's porpoise sighted ($i = 1 \dots I$): the perpendicular distance between the group and the transect line (x_i); estimated group size (s_i) based on the average of best estimates recorded independently by observers for each sighting, and estimated Beaufort sea state at the time of the sighting (B_i).

2.2 | Habitat covariates

For all three BHM, we estimated a series of density–habitat relationships incorporating various combinations of habitat covariates: a static covariate (depth) and a dynamic covariate (sea-surface temperature, SST). The choice of habitat covariates drew on previous habitat models for Dall's porpoise using generalized additive models (e.g., Becker et al., 2010, 2014; Forney, 2000). Data on habitat covariates were compiled for each transect segment and for a set of 1/3-degree grid cells encompassing the CCE survey region and the broader region, R (Figure 1a). Spatial and temporal scales were chosen to capture broad habitat features and the distribution of water masses rather than fine-scale features (see Becker et al., 2010).

2.2.1 | Bathymetric data

Bathymetric data were derived from the ETOPO1 1 arc-minute global relief model (Amante & Eakins, 2009). For each 1/3-degree grid cell, the average water depth (m) was calculated as the mean of all negative depth values within the grid cell. For each transect segment, the average water depth was calculated as the mean of all negative depth values within a 1/3-degree grid cell centred on the segment mid-point (Figure 1b).

2.2.2 | Sea-surface temperature

Sea-surface temperature (SST) data were derived from the AVHRR Pathfinder version 5.0 monthly full-resolution data set (NOAA NMFS SWFSC ERD 2010, downloaded from <http://coastwatch.pfeg.noaa.gov/data.html>). For each 1/3-degree grid cell, the average SST (°C) for each survey month was calculated as the mean of all monthly SST values for the relevant month within the grid cell. For each transect segment, the average SST for the segment date was calculated as the mean of all monthly SST values for the relevant month within a 1/3-degree grid cell centred on the segment mid-point (Figure 1c–g).

2.3 | Group size

Preliminary analysis (see Appendix S1) did not show interannual variation in the distribution of Dall's porpoise group sizes, consistent with previous findings based on generalized additive models by Barlow (2015). We therefore assumed a constant group size distribution and used group as the basic unit for the remainder of the analysis. ("Individual" could be substituted for "group" for application to species that occur primarily as single individuals.)

2.4 | Observation submodel

For all three BHM, the observation submodel involves the same two likelihoods: (1) the likelihood of the distances of detected groups from the transect line, and (2) the likelihood of the number of groups detected along transect segments. Both likelihoods are based on standard distance sampling theory (Buckland et al., 2001).

2.4.1 | Likelihood of the distances of detected groups from the transect line

We assumed a half-normal detection function, $g(x) \sim \text{half-} N(0, \sigma^2)$, truncated at a maximum detection distance, x_{max} . As in standard distance sampling theory (Buckland et al., 2001), we also assumed that the distribution of groups at local scales followed a homogenous Poisson distribution, such that the perpendicular distances from the transect line of all groups within the maximum detection distance (including undetected groups) were uniformly distributed, i.e. $x \sim U(0, x_{\text{max}})$. Given this assumption of local homogeneity, the probability density function of the distances of detected groups, $f(x)$, is the same shape as the detection function $g(x)$, but rescaled so that it integrates to 1. The likelihood of distances of detected groups is therefore:

$$x_i \sim N(0, \sigma_i^2) T(0, x_{\text{max}}) \quad (1)$$

where $T(0, x_{\text{max}})$ denotes truncation at 0 and x_{max} . We set x_{max} to 4 km for Dall's porpoise, following Barlow (2015). Preliminary analysis (see Appendix S1) indicated greatest support for modelling the scale parameter of the detection function, σ_i^2 , as a linear function of Beaufort

sea state. We therefore used the following equation for the remainder of the analysis:

$$\sigma_i = a_0 + a_1 \cdot B_i. \quad (2)$$

2.4.2 | Likelihood of the number of groups detected along transect segments

Preliminary analysis of the likelihood of the number of groups detected along each transect segment, y_j , indicated greater support for the negative binomial over the Poisson distribution. The analysis presented below was therefore based on the negative binomial distribution. The expected number of detected groups, λ_j , depends on the local group density, D_j , the segment length, L_j , the effective strip half-width, ESW_j , and the detection probability on the transect line, $g_j(0)$:

$$\lambda_j = D_j \cdot 2 \cdot L_j \cdot ESW_j \cdot g_j(0) \quad (3)$$

where the effective strip half-width is calculated from the probability density of the detected distances, $ESW_j = 1/f_j(0)$. This is a simple re-arrangement of the conventional distance sampling equation (Buckland et al., 2001; see also Barlow, 2015):

$$D_j = \frac{\lambda_j \cdot f_j(0)}{2 \cdot L_j \cdot g_j(0)}. \quad (4)$$

Given truncation at x_{\max} ,

$$f_j(0) = \frac{\varphi(0 | 0, \sigma_j^2)}{\{\Phi(x_{\max} | 0, \sigma_j^2) - 0.5\}} \quad (5)$$

where $\varphi(x | 0, \sigma^2)$ is the density at x of the normal distribution with zero mean and variance σ^2 , and the denominator is the cumulative density of the normal distribution between 0 and x_{\max} . The scale parameter, σ_j^2 , is estimated as in Equation 2, given the average Beaufort sea state along each transect segment, B_j .

Preliminary analysis of the detection probability on the transect line, $g_j(0)$, indicated that it declined as a quadratic function of Beaufort sea state (see Appendix S1). We therefore used the following equation for the remainder of the analysis:

$$g_j(0) = 1 + b_1 \cdot B_j + b_2 \cdot B_j^2. \quad (6)$$

The intercept was set to 1 so that $g(0) = 1$ at Beaufort 0, following Barlow (2015).

Dall's porpoise may be attracted to survey vessels leading to a positive bias in abundance estimates. However, Barlow (1995) found that most Dall's porpoise in the 1991 survey were sighted using 25× binoculars before showing any apparent reaction to the vessel and concluded that vessel attraction was not a major issue for Dall's porpoise in the CCE given the survey protocol used in 1991 and all subsequent surveys used in this analysis.

2.5 | Population process submodel

2.5.1 | Models H1a and H1b: Population dynamics submodel

The population dynamics submodel is based on a discrete Markovian exponential growth model:

$$\begin{aligned} \text{At } t=1, N_t &\sim \text{discrete uniform}(0, N_{\max}) \\ \text{For } t=2 \dots T, N_t &= N_{t-1} \cdot e^{(u+\eta_t)} \quad \text{where } \eta_t \sim \text{Normal}(0, Q) \end{aligned} \quad (7)$$

where N_t is the number of groups in year t . There are three estimated parameters: initial population size, N_1 ; the constant trend, u ; and the interannual process variance, Q . N_{\max} is a user-defined upper bound and should be increased if estimated values approach this limit.

For the spatially closed model (Model H1a), interannual population dynamics are estimated for a population that is restricted to the CCE survey region; whereas, for the spatially open model (Model H1b), population dynamics are estimated for a population that extends to the broader region, R .

2.6 | Distribution process submodels

2.6.1 | Model H0: Mixed-effects density distribution submodel

In the mixed-effects model, the relationship between group densities and habitat covariates is assumed constant in terms of fixed effects, while random effects on year allow for additional interannual variation in densities. The expected density of groups D along each transect segment j in each month m and year t depends on habitat conditions at that location only, independent of habitat available elsewhere. For example:

$$D_{j,m,t} = \exp(\alpha_0 + \alpha \cdot \mathbf{Z}_{j,m,t} + \varepsilon_t) \quad (8)$$

where \mathbf{Z} refers to some vector of habitat covariates, and $\varepsilon_t \sim \text{Normal}(0, \Omega)$ represents random effects on year. Various combinations of habitat covariates were explored (see Results).

2.6.2 | Models H1a and H1b: Ideal free redistribution submodel

In the ideal free redistribution submodel, the population is assumed to distribute itself throughout its range in proportion to relative habitat suitability in each secondary sampling period (i.e. each survey month in this case). The expected density of groups D along each segment j within each grid cell k , $j(k)$, thus depends on habitat suitability h in grid cell k relative to habitat suitability over all $k = 1 \dots K$ grid cells in the range in each secondary sampling period. For example:

$$h_{j,m,t} = \exp(\alpha_0 + \alpha \cdot \mathbf{Z}_{j,m,t}) \quad (9)$$

$$D_{j(k),m,t} = N_t \cdot h_{k,m,t} / \sum_1^K (h_{k,m,t} \cdot A_k) \quad (10)$$

where A_k represents the area of each grid cell. For the spatially closed model (Model H1a), the range is the CCE survey region; for the spatially open model (Model H1b), the range is the broader region, R , and thus involves extrapolation beyond the observed distance sampling data. Various combinations of habitat covariates were explored (see Results).

2.7 | Model implementation and comparison

The three BHM models were estimated using Markov chain Monte Carlo methods implemented in JAGS (Plummer, 2003) to sample from the posterior distributions (see Supporting Information Appendix S3 for sample model code). Prior distributions for stochastic parameters were generally non-informative (see Appendix S2). Bounds on parameters for the detection function were set in line with distance sampling theory.

Five hundred parameter sets were saved from each of two chains with a thinning rate of 100, and convergence was checked visually and using standard diagnostics including the Geweke and Gelman-Rubin statistics (Gelman & Rubin, 1992; Geweke, 1992). The relative estimation performance of the three BHM models and the contribution of habitat data were evaluated using Watanabe's Information Criterion (WAIC, Watanabe, 2010; Vehtari, Gelman, & Gabry, 2016).

3 | RESULTS

3.1 | Population and distribution processes

We used the BHM models to investigate relative support for the two main hypotheses for population and distribution processes in the case of Dall's porpoise (i.e. Models H0 vs H1). Model comparison using WAIC indicated similar levels of support for the null model (i.e. the model version without environmental covariates in the distribution model) across all three BHM models, as expected (Table 1). WAIC also indicated similar levels of support for the depth-only models across all three

BHM models, as expected because depth is a static covariate. Differences in the levels of support for the three BHM models emerged once the dynamic covariate, SST, was introduced into the models. For models incorporating SST, WAIC indicated consistently greater levels of support for the two ideal free redistribution models (Models H1a and H1b) over the conventional mixed-effects model (Model H0). More complex versions of the conventional model (i.e. versions including a quadratic function of SST) exhibited poor MCMC mixing of parameters on SST even at high thinning rates, providing further indications that the conventional model is misspecified.

When the two ideal free redistribution models were compared, WAIC generally indicated similar levels of support for the restricted range model (Model H1a) and the extended range model (Model H1b).

For all three BHM models, model comparison using WAIC indicated strong support for incorporating habitat information (Table 1). For both the restricted range and extended range ideal free redistribution models (Models H1a and H1b), the versions with greatest support based habitat suitability on quadratic functions of both depth and SST. These two models received substantially greater support than any of the other models.

3.2 | Estimates of population size and trends

We also examined the potential for IPRMs that combine an aggregate population dynamics submodel with a habitat-based redistribution submodel to strengthen estimation of population size and trends for species with dynamic spatial distributions, such as Dall's porpoise. We focus on the results for the restricted range model (Model H1a) because it provides a single estimate of population size in the CCE survey region in each survey year rather than a seasonally varying abundance estimate. Figure 2 shows posterior distributions for the three parameters in the restricted range IPRM population submodel, comparing the null model (which is the same for all BHM models) and the full habitat model (i.e. quadratic functions of both depth and SST). The initial population size and the long-term trend were both estimated more precisely and the population process variance was lower in the full habitat model compared to the null model.

TABLE 1 Model comparison based on differences in Watanabe's information criterion (Δ WAIC)

	Δ WAIC		
	H0. Conventional (mixed effects)	H1a. IPRM (ideal free redistribution; restricted range)	H1b. IPRM (ideal free redistribution; extended range)
Null	555	555	555
Depth	442	442	442
Depth ²	362	362	362
SST	160	132	142
SST + depth	160	135	143
SST ²	89	41	39
SST ² + depth	84	41	40
SST ² + depth ²	29	2.4	0.0

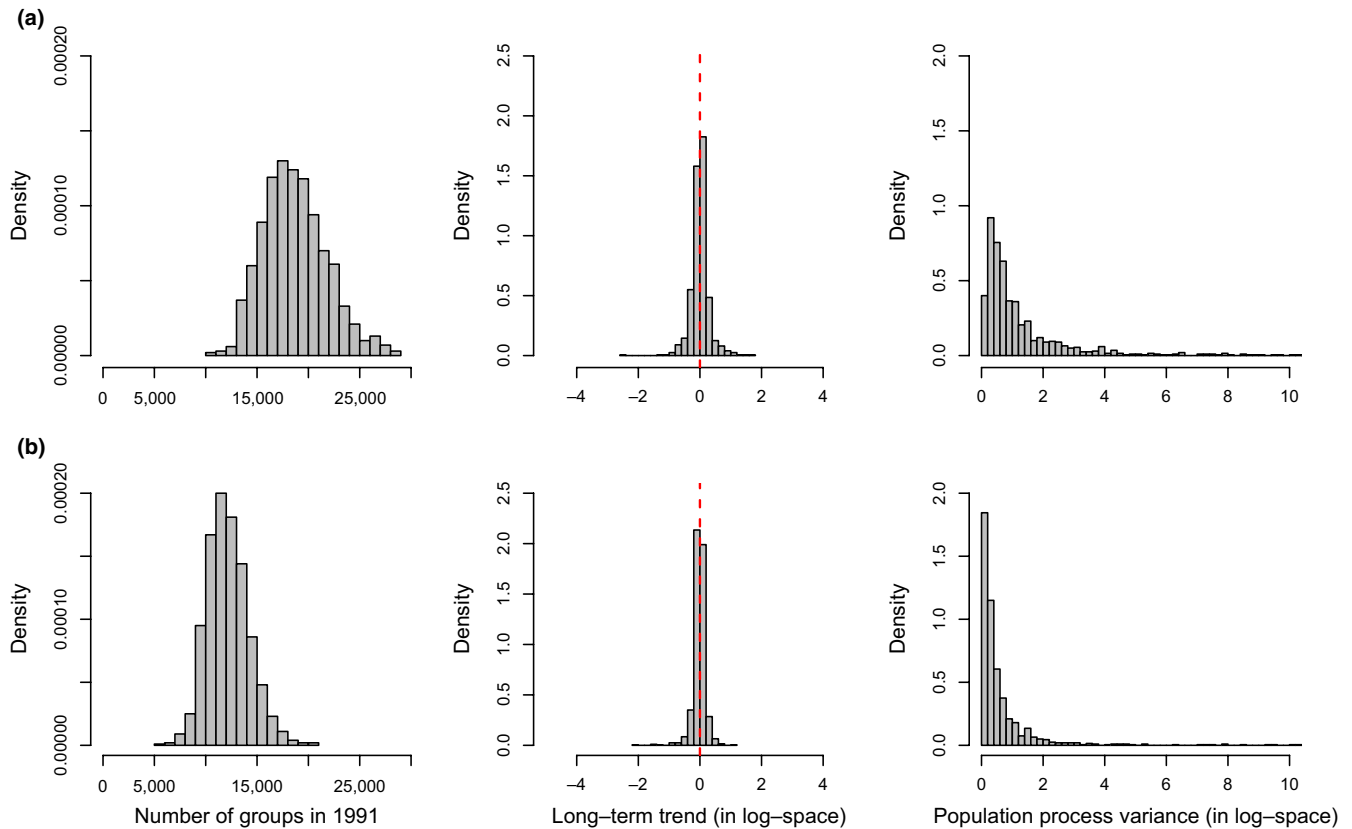


FIGURE 2 Posterior distributions for the initial population size (number of groups in 1991), long-term trend (in log-space) and the population process variance (in log-space) for the restricted range IPRM (Model H1a), for (a) the null model and (b) the full habitat model. [Colour figure can be viewed at wileyonlinelibrary.com]

The estimated population dynamics are similar between the null and the full habitat model, but the full habitat model leads to less interannual variability in population size estimates and reduced uncertainty (Figure 3). In both cases, the credible intervals tend to expand during non-survey years.

4 | DISCUSSION

4.1 | Population and distribution processes

The three BHM represent distinct hypotheses about variation in the abundance and distribution patterns of Dall's porpoise within the CCE survey region. The ideal free redistribution models (Models H1a and H1b) are based on explicit, ecologically plausible, mechanistic population and distribution processes. The strong support for these models is consistent with the hypothesis that the summer/fall distribution of Dall's porpoise expands and contracts in line with the distribution of suitable habitat in each year, leading to lower densities in suitable habitat when suitable habitat is extensive and higher densities when it is more restricted, despite stable population sizes. These results are in line with the suggestion by Henderson et al. (2014) that a positive relationship between Dall's porpoise sightings per unit effort in southern California and the Pacific Decadal Oscillation might be explained by the concentration of Dall's porpoise in the remaining cool

productive waters relatively close to shore (see also Benson, Croll, Marinovic, Chavez, & Harvey, 2002).

The restricted range and extended range ideal free redistribution models (Models H1a and H1b) received similar levels of support from the Dall's porpoise data, even though the restricted range model implies a stable population in the CCE survey region during each survey season, while the spatially open model allows for seasonal variation in the proportion of the population within the survey region. In this case, the results for extended range model indicated fairly limited seasonal variation in the proportion of the population in the CCE survey region (Figure 4), suggesting that the amount of suitable habitat in the survey region was generally closely correlated with the amount of suitable habitat in the broader region, which explains the similar levels of support for the restricted and extended range models.

Conversely, the conventional mixed-effects model (Model H0), which received substantially less support, implies substantial inflows and outflows of Dall's porpoise into the CCE survey region in all years, with a reduction in abundance during the summer as the amount of suitable habitat in the survey region decreases and an increase in fall (Figure 4). In years when the extended range ideal free redistribution model (Model H1b) indicates more pronounced seasonal variation (e.g., 1996 and 2005), the predicted patterns differ from the conventional model. The extended range ideal free redistribution model indicates an increase in the number of groups in the CCE survey region in August

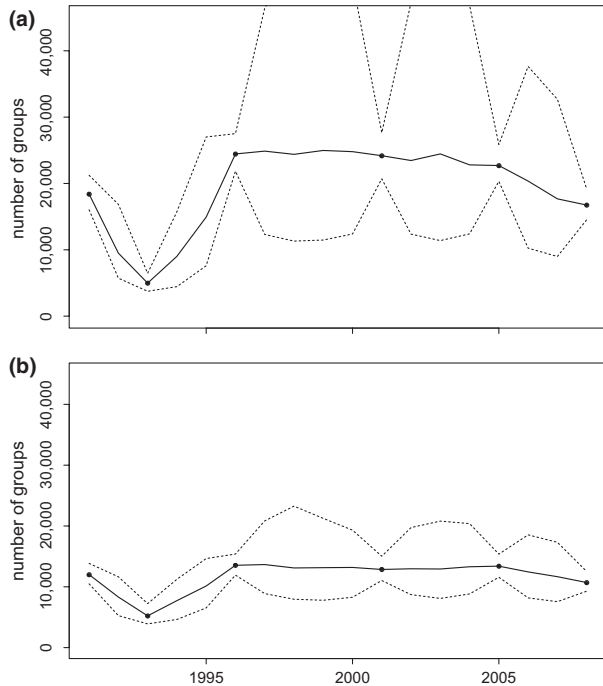


FIGURE 3 Estimated population size within the California Current Ecosystem survey region over the study period based on the restricted range integrated population-redistribution model (Model H1a) for (a) the null model and (b) the full habitat model. The solid line represents the median; dotted lines represent the 20th and 80th percentiles; points indicate survey years

and September of 1996 and 2005, suggesting that the proportion of suitable habitat in the survey region was high relative to the broader region R in the summers of 1996 and 2005. This contrasts with the conventional mixed-effects model, which indicates a decrease in the number of groups in the survey region in August and September in all years.

The implication of the strong support for the ideal free redistribution hypothesis for Dall's porpoise and the contrasting seasonal variation patterns is that conventional models (such as Model H0) that assume a constant relationship between densities and habitat within each survey year would be expected to give highly variable and uncertain abundance estimates.

4.2 | Incorporating habitat into estimates of population size and trends

Integrated population-distribution models, such as those developed here, have several advantages for estimating population size when compared to conventional approaches. First, the IPRM uses information from all surveys to estimate the population size in each survey year, rather than treating the population size in each year as independent. In this way, the model "borrows" information from previous and subsequent years, leading to less variable and more precise estimates of population size (see also Moore & Barlow, 2013). Second, when a population process and distribution process submodel are combined within the same model, variation in estimated densities is

partitioned into two distinct sources of variation: changes in population size and changes in distribution patterns attributable to variation in habitat covariates. This leads to lower estimates of population process variance for species with dynamic spatial distributions linked to variation in the habitat distribution. Models that do not account for variation in distribution patterns may overestimate variability in population processes (Forney, 2000). Figure 5 provides a comparison of previous estimates of the population size of Dall's porpoise in the CCE survey region for 1996, 2001, 2005 and 2008 (Barlow, 2016) versus estimates based on the full habitat restricted range IPRM. IPRM estimates fall well within the range of the previous estimates, except for 2001. The higher IPRM estimate in this year reflects the reduced variability in population processes in models that incorporate an explicit population process and allow for uncertainty in the observation model. Finally, the IPRM provides valuable information for interpreting variation in population size within a survey region in terms of real changes in abundance, which may be a management concern, versus shifts in distribution.

5 | CONCLUSIONS

The analysis presented here demonstrates a new ecologically realistic approach for estimating population size and trends for cetaceans and other highly mobile species. Future assessments of population size and trends of cetaceans and other highly mobile species with dynamic spatial distributions could be improved by using integrated population-distribution models that incorporate habitat covariates. For species with distributions linked to variation in the distribution of suitable habitat, we strongly recommend considering models that allow populations to adjust their relationship to habitat covariates depending on the availability of suitable habitat, such as those developed here. In particular, this modelling approach could be readily applied to other cetacean and seabird species whose abundance is estimated using distance sampling or strip transect survey methods (e.g., Ballance, 2007; Forney, 2000). Pinnipeds are generally more cryptic at sea, but aerial surveys are used to estimate abundance of seals resting on highly dynamic sea ice platforms (e.g., Conn et al., 2015). On land, this modelling approach is most relevant to highly mobile species that depend on spatio-temporally variable habitats that can be monitored through remote sensing, such as herbivores and their predators in semi-arid rangeland ecosystems (e.g., Augustine, 2010; Blaum, Rossmannith, Schwager, & Jeltsch, 2007).

ACKNOWLEDGEMENTS

The California Current Ecosystem survey data used in this analysis were collected by a large dedicated team from NOAA's Southwest Fisheries Science Center. We thank the cruise leaders, marine mammal observers, survey coordinators, ships' officers and crew who all contributed to collecting these data. We also thank M. Kéry, A. Zerbini and an anonymous reviewer for their thoughtful comments and suggestions on the manuscript.

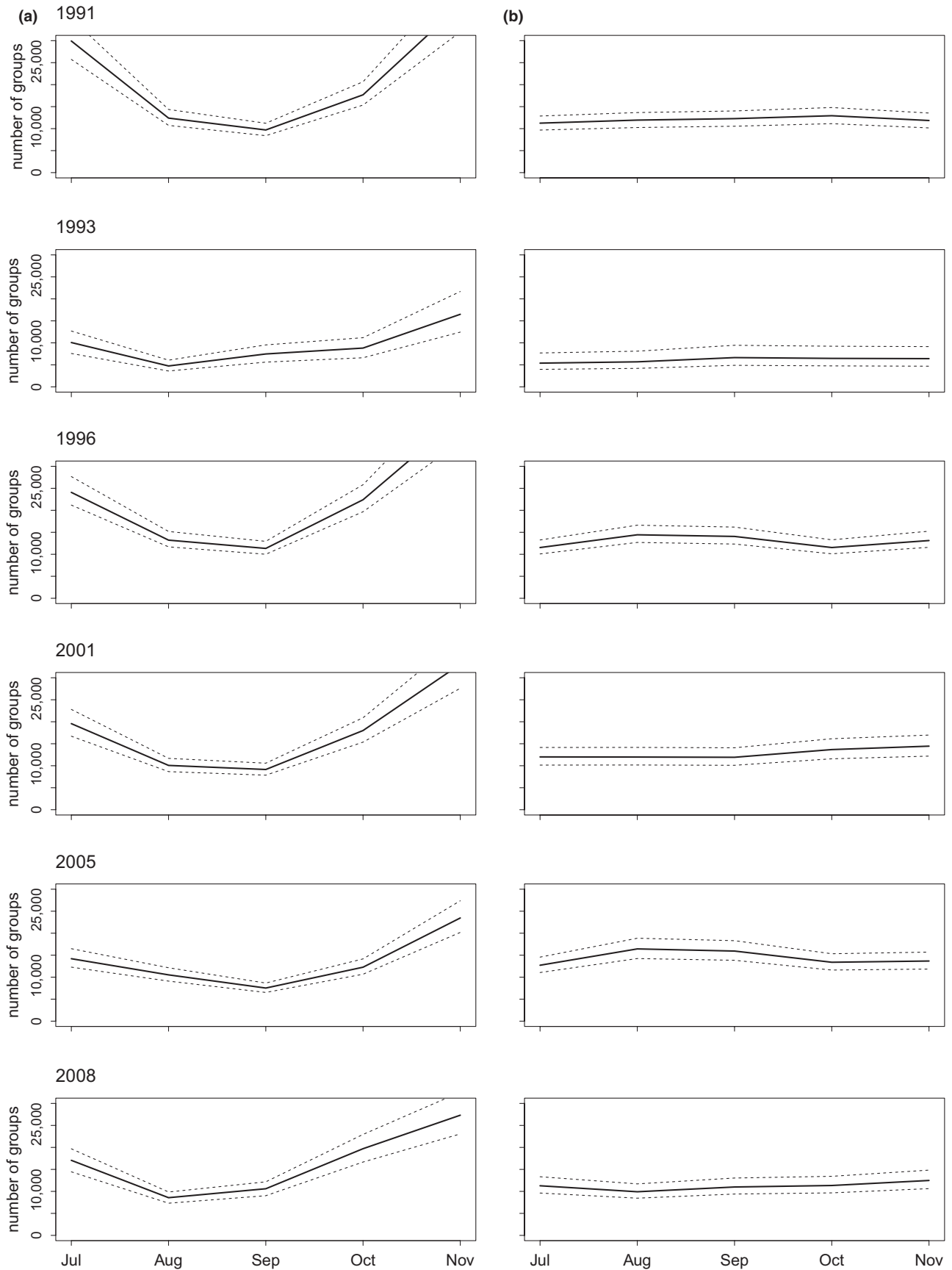


FIGURE 4 Seasonal variation in number of groups within the survey region estimated by (a) the mixed-effects full habitat model (Model H0), and (b) the extended range IPRM full habitat model (Model H1b). The solid line represents the median; dotted lines represent the 20th and 80th percentiles

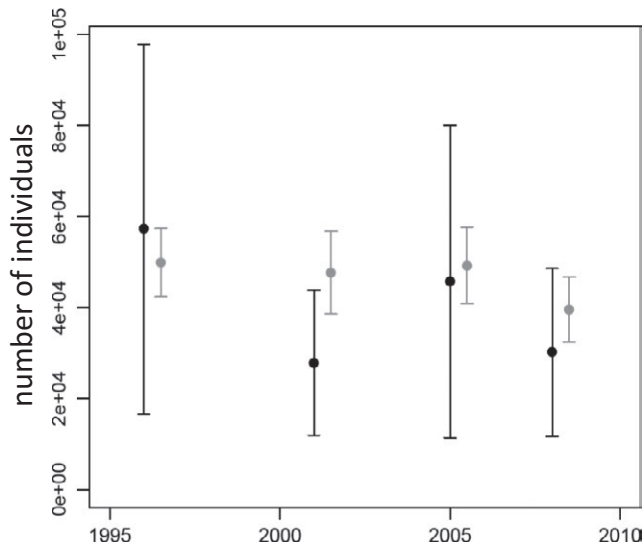


FIGURE 5 Comparison of previous estimates of the population size of Dall's porpoise in the California Current Ecosystem survey region in 1996, 2001, 2005 and 2008 (Barlow, 2016, table 8) shown in black versus estimates based on the full habitat restricted range integrated population-redistribution model shown in grey. Points indicate the mean abundance estimate in each year; error bars indicate ± 1 SD

DATA ACCESSIBILITY

NOAA's Southwest Fisheries Science Center cetacean sightings and survey effort can be accessed freely on OBIS SEAMAP (<http://seamap.env.duke.edu/>). Bathymetric data were derived from the ETOPO1 1 arc-minute global relief model (Amante & Eakins, 2009) and are available for download at <https://www.ngdc.noaa.gov/mgg/global/relief/ETOPO1/data/>. Sea-surface temperature (SST) data were derived from the AVHRR Pathfinder version 5.0 monthly full-resolution data set (NOAA NMFS SWFSC ERD 2010) and are available for download at <http://coastwatch.pfeg.noaa.gov/data.html>.

ORCID

Charlotte Boyd  <http://orcid.org/0000-0003-4095-9390>

REFERENCES

- Amante, C., & Eakins, B. W. (2009). *ETOPO1 1 arc-minute global relief model: Procedures, data sources and analysis*. NOAA Technical Memorandum NESDIS NGDC-24. Boulder, CO: National Geophysical Data Center.
- Augustine, D. J. (2010). Response of native ungulates to drought in semi-arid Kenyan rangeland. *African Journal of Ecology*, *48*, 1009–1020.
- Ballance, L. T. (2007). Understanding seabirds at sea: Why and how. *Marine Ornithology*, *35*, 127–135.
- Barlow, J. (1995). The abundance of cetaceans in California waters. Part I: Ship surveys in summer and fall of 1991. *Fishery Bulletin*, *93*, 1–14.
- Barlow, J. (2015). Inferring trackline detection probabilities, $g(0)$, for cetaceans from apparent densities in different survey conditions. *Marine Mammal Science*, *31*, 923–943.
- Barlow, J. (2016). *Cetacean abundance in the California Current estimated from ship-based line-transect surveys in 1991–2014*. NOAA Administrative Report LJ-16-01. La Jolla, CA, USA: National Marine Fisheries Service.
- Barlow, J., & Forney, K. A. (2007). Abundance and population density of cetaceans in the California Current ecosystem. *Fishery Bulletin*, *105*, 509–526.
- Becker, E. A., Forney, K. A., Ferguson, M. C., Foley, D. G., Smith, R. C., Barlow, J., & Redfern, J. V. (2010). Comparing California Current cetacean-habitat models developed using in situ and remotely sensed sea surface temperature data. *Marine Ecology Progress Series*, *413*, 163–183.
- Becker, E. A., Forney, K. A., Foley, D. G., Smith, R. C., Moore, T. J., & Barlow, J. (2014). Predicting seasonal density patterns of California cetaceans based on habitat models. *Endangered Species Research*, *23*, 1–22.
- Benson, S. R., Croll, D. A., Marinovic, B. B., Chavez, F. P., & Harvey, J. T. (2002). Changes in the cetacean assemblage of a coastal upwelling ecosystem during El Niño 1997–98 and La Niña 1999. *Progress in Oceanography*, *54*, 279–291.
- Blaum, N., Rossmannith, E., Schwager, M., & Jeltsch, F. (2007). Responses of mammalian carnivores to land use in arid savanna rangelands. *Basic and Applied Ecology*, *8*, 552–564.
- Buckland, S. T., Anderson, D. R., Burnham, K. P., Laake, J. L., Borchers, D. L., & Thomas, L. (2001). *Introduction to distance sampling: Estimating abundance of biological populations*. Oxford, U.K.: Oxford University Press.
- Calambokidis, J., & Barlow, J. (2004). Abundance of blue and humpback whales in the eastern North Pacific estimated by capture-recapture and line-transect methods. *Marine Mammal Science*, *20*, 63–85.
- Carretta, J. V., Forney, K. A., Oleson, E. M., Weller, D. W., Lang, A. R., Baker, J., ... Brownell, R. L. Jr (2017). U.S. Pacific Marine Mammal Stock Assessments: 2016. U.S. Department of Commerce, NOAA Technical Memorandum, NOAA-TM-NMFS-SWFSC-577. 407 p.
- Chavez, F. P., Ryan, J., Lluch-Cota, S. E., & Niquen, M. (2003). From anchovies to sardines and back: Multidecadal change in the Pacific Ocean. *Science*, *299*, 217–221.
- Chelgren, N. D., Samora, B., Adams, M. J., & McCreary, B. (2011). Using spatiotemporal models and distance sampling to map the space use and abundance of newly metamorphosed western toads (*Anaxyrus boreas*). *Herpetological Conservation and Biology*, *6*, 175–190.
- Conn, P. B., Johnson, D. S., Hoef, J. M. V., Hooten, M. B., London, J. M., & Boveng, P. L. (2015). Using spatiotemporal statistical models to estimate animal abundance and infer ecological dynamics from survey counts. *Ecological Monographs*, *85*, 235–252.
- Evans, P. G. H., & Hammond, P. S. (2004). Monitoring cetaceans in European waters. *Mammal Review*, *34*, 131–156.
- Forney, K. A. (2000). Environmental models of cetacean abundance: Reducing uncertainty in population trends. *Conservation Biology*, *14*, 1271–1286.
- Forney, K. A., & Barlow, J. (1998). Seasonal patterns in the abundance and distribution of California cetaceans, 1991–1992. *Marine Mammal Science*, *14*, 460–489.
- Forney, K. A., Ferguson, M. C., Becker, E. A., Fiedler, P. C., Redfern, J. V., Barlow, J., ... Ballance, L. T. (2012). Habitat-based spatial models of cetacean density in the eastern Pacific Ocean. *Endangered Species Research*, *16*, 113–133.
- Fretwell, S. D., & Lucas, H. L. (1970). On territorial behavior and other factors influencing habitat distribution in birds. I. Theoretical development. *Acta Biotheoretica*, *19*, 16–36.
- Gelman, A., & Rubin, D. B. (1992). Inference from iterative simulation using multiple sequences. *Statistical Science*, *7*, 457–511.
- Gerrard, T., & Eguchi, T. (2011). Precautionary design of a marine protected area based on a habitat model. *Endangered Species Research*, *15*, 159–166.
- Geweke, J. (1992). Evaluating the accuracy of sampling-based approaches to calculating posterior moments. In J. M. Bernardo, J. O. Berger, A. P. Dawid, & A. F. M. Smith (Eds.), *Bayesian statistics 4* (pp. 169–193). Oxford: Oxford University Press.

- Gregoire, T. G. (1998). Design-based and model-based inference in survey sampling: Appreciating the difference. *Canadian Journal of Forest Research-Revue Canadienne De Recherche Forestiere*, 28, 1429–1447.
- Henderson, E. E., Forney, K. A., Barlow, J. P., Hildebrand, J. A., Douglas, A. B., Calambokidis, J., & Sydeman, W. J. (2014). Effects of fluctuations in sea-surface temperature on the occurrence of small cetaceans off Southern California. *Fishery Bulletin*, 112, 159–177.
- Jefferson, T. A. (1988). *Phocoenoides dalli*. *Mammalian Species*, 319, 1–7.
- Johnson, D. S., Laake, J. L., & Hoef, J. M. V. (2010). A model-based approach for making ecological inference from distance sampling data. *Biometrics*, 66, 310–318.
- Kinzey, D., Olson, P., & Gerrodette, T. (2000). *Marine mammal data collection procedures on research ship line-transect surveys by the Southwest Fisheries Science Center*. NOAA Administrative Report LJ-00-08. La Jolla, CA, USA: National Marine Fisheries Service.
- Levin, S. A. (1992). The problem of pattern and scale in ecology. *Ecology*, 73, 1943–1967.
- Moore, J. E., & Barlow, J. (2011). Bayesian state-space model of fin whale abundance trends from a 1991–2008 time series of line-transect surveys in the California Current. *Journal of Applied Ecology*, 48, 1195–1205.
- Moore, J. E., & Barlow, J. P. (2013). Declining abundance of beaked whales (Family Ziphiidae) in the California Current large marine ecosystem. *PLoS ONE*, 8, e52770.
- Moore, J. E., & Barlow, J. P. (2014). Improved abundance and trend estimates for sperm whales in the eastern North Pacific from Bayesian hierarchical modeling. *Endangered Species Research*, 25, 141–150.
- Nadeem, K., Moore, J. E., Zhang, Y., & Chipman, H. (2016). Integrating population dynamics models and distance sampling data: A spatial hierarchical state-space approach. *Ecology*, 97, 1735–1745.
- Nandintsetseg, D., Kaczensky, P., Ganbaatar, O., Leimgruber, P., & Mueller, T. (2016). Spatiotemporal habitat dynamics of ungulates in unpredictable environments: The khulan (*Equus hemionus*) in the Mongolian Gobi desert as a case study. *Biological Conservation*, 204, 313–321.
- Oedekoven, C. S., Buckland, S. T., Mackenzie, M. L., King, R., Evans, K. O., & Burger, L. W. (2014). Bayesian methods for hierarchical distance sampling models. *Journal of Agricultural Biological and Environmental Statistics*, 19, 219–239.
- Pardo, M. A., Gerrodette, T., Beier, E., Gendron, D., Forney, K. A., Chivers, S. J., ... Palacios, D. M. (2015). Inferring cetacean population densities from the absolute dynamic topography of the ocean in a hierarchical Bayesian framework. *PLoS ONE*, 10, e0120727.
- Plummer, M. (2003). *JAGS: a program for analysis of Bayesian graphical models using Gibbs sampling*. In: *Proceedings of the 3rd International Workshop on Distributed Statistical Computing*, Vienna, Austria.
- Royle, J. A., Dawson, D. K., & Bates, S. (2004). Modeling abundance effects in distance sampling. *Ecology*, 85, 1591–1597.
- Royle, J. A., & Dorazio, R. M. (2008). *Hierarchical modeling and inference in ecology*. Amsterdam: Academic Press.
- Royle, J. A., Nichols, J. D., Karanth, K. U., & Gopalaswamy, A. M. (2009). A hierarchical model for estimating density in camera-trap studies. *Journal of Applied Ecology*, 46, 118–127.
- Santora, J. A., Schroeder, I. D., Field, J. C., Wells, B. K., & Sydeman, W. J. (2014). Spatio-temporal dynamics of ocean conditions and forage taxa reveal regional structuring of seabird-prey relationships. *Ecological Applications*, 24, 1730–1747.
- Sillett, T. S., Chandler, R. B., Royle, J. A., Kéry, M., & Morrison, S. A. (2012). Hierarchical distance-sampling models to estimate population size and habitat-specific abundance of an island endemic. *Ecological Applications*, 22, 1997–2006.
- Stevick, P. T., McConnell, B. J., & Hammond, P. S. (2002). Patterns of movement. In A. R. Hoelzel (Ed.), *Marine mammal biology: An evolutionary approach* (pp. 185–216). Oxford: Blackwell.
- Taylor, B. L., Wade, P. R., De Master, D. P., & Barlow, J. (2000). Incorporating uncertainty into management models for marine mammals. *Conservation Biology*, 14, 1243–1252.
- Torres, L. G., Read, A. J., & Halpin, P. (2008). Fine-scale habitat modeling of a top marine predator: Do prey data improve predictive capacity? *Ecological Applications*, 18, 1702–1717.
- Tynan, C. T., Ainley, D. G., Barth, J. A., Cowles, T. J., Pierce, S. D., & Spear, L. B. (2005). Cetacean distributions relative to ocean processes in the northern California Current System. *Deep-Sea Research Part II-Topical Studies in Oceanography*, 52, 145–167.
- Vehtari, A., Gelman, A., & Gabry, J. (2016). Practical Bayesian model evaluation using leave-one-out cross-validation and WAIC. *Statistics and Computing*, 27, 1413–1432.
- Wade, P. R. (1998). Calculating limits to the allowable human-caused mortality of cetaceans and pinnipeds. *Marine Mammal Science*, 14, 1–37.
- Watanabe, S. (2010). Asymptotic equivalence of Bayes cross validation and widely applicable information criterion in singular learning theory. *Journal of Machine Learning Research*, 11, 3571–3594.

BIOSKETCH

The authors are interested in understanding how the seasonal abundance and distribution of cetaceans and other highly mobile marine species relate to the prey availability and underlying biological and physical habitat features. They conduct applied research on a wide range of species to address specific conservation and management questions. Core activities include assessing cetacean population size, trends and distributions, and providing scientific information to guide strategies for reducing the effects of fishing operations and other human activities on protected species.

Author contributions: C.B. conceived the ideas and developed the modelling approach with input from J.B., E.A.B., K.A.F., T.G., J.E.M and A.E.P; J.B., K.A.F and T.G designed and led the vessel-based survey cruises that collected the cetacean survey data; E.A.B. and K.A.F. processed the cetacean survey data; C.B. processed the environmental covariate data, analysed the data, and led the writing; J.P.B., E.A.B., K.A.F., T.G., J.E.M and A.E.P. reviewed the analysis, helped interpret the results and reviewed the final manuscript.

SUPPORTING INFORMATION

Additional Supporting Information may be found online in the supporting information tab for this article.

How to cite this article: Boyd C, Barlow J, Becker EA, et al. Estimation of population size and trends for highly mobile species with dynamic spatial distributions. *Divers Distrib*. 2018;24:1–12. <https://doi.org/10.1111/ddi.12663>